metals

MDPI

Article

Comparative Study on Combustion Behavior of Aluminum-Based Alloy Fuels and Aluminum Powder in Solid Propellants

Haoyue Xin [1], Kun Wang [1,2], Hui Ren [1,*] and Qingjie Jiao [1]

[1] State Key Laboratory of Explosion of Science and Technology, Beijing Institute of Technology, Beijing 100081, China; 3120220262@bit.edu.cn (H.X.); wangkun_k@sohu.com (K.W.); jqj@bit.edu.cn (Q.J.)
[2] Inner Mongolia Synthetic Chemical Research Institute, Hohhot 010011, China
* Correspondence: renhui@bit.edu.cn; Tel.: +86-135-2153-8722

Abstract: In order to reduce the ignition temperature and improve the combustion efficiency of aluminum powder, three aluminum-based alloy fuels, Al–Mg, Al–Zn, and Al–Si–Mg, were prepared by the atomization method. The oxidation, ignition, and combustion performance of alloy fuels were investigated, and the results showed that, using pure aluminum powder as a reference, the weight gain of alloy fuels increased from 10% to 84%, the reaction activation energy decreased from 582 kJ·mol^{-1} to 208 kJ·mol^{-1}, the alloy fuels containing Mg had good ignition response, and aluminum-based alloy fuels showed high calorific value and efficient combustion as a whole. In order to investigate the combustion behavior of alloy fuels in the solid propellant, tests were conducted on the mechanics, safety, process, and combustion properties of propellant according to the national standard, and the test results showed that, compared with the propellant made of aluminum powder with same quality, the propellant made of alloy has better mechanical properties, higher frictional sensitivity, lower electrostatic sensitivity, comparable process performance, and increased combustion calorific value and combustion speed. Engine test results confirmed that Al–Zn and Al–Si–Mg alloy fuels could effectively improve the specific impulse efficiency of the solid propellant and reduced the residual rate of the engine.

Keywords: aluminum-based alloy fuel; aluminum powder; solid propellant; application; combustion

check for updates

Citation: Xin, H.; Wang, K.; Ren, H.; Jiao, Q. Comparative Study on Combustion Behavior of Aluminum-Based Alloy Fuels and Aluminum Powder in Solid Propellants. *Metals* **2023**, *13*, 1492. https://doi.org/10.3390/met13081492

Academic Editor: Arne Mattias Thuvander

Received: 25 July 2023
Revised: 14 August 2023
Accepted: 17 August 2023
Published: 20 August 2023

Copyright: © 2023 by the authors. Licensee MDPI, Basel, Switzerland. This article is an open access article distributed under the terms and conditions of the Creative Commons Attribution (CC BY) license (https://creativecommons.org/licenses/by/4.0/).

1. Introduction

Hydroxyl-terminated polybutadiene composite solid propellant (HTPB propellant) is based on hydroxyl-terminated polybutadiene (HTPB), ammonium perchlorate (AP), and aluminum (Al) as raw materials, which have good mechanical, safety, and process properties, and also have the advantages of moderate energy level, stable ballistic performance, and low cost, etc. It is widely used in strategic and tactical models as well as solid engine charges in aerospace [1–4]. As one of the main components of HTPB propellant, aluminum has high combustion heat and density, which can significantly improve the energy and density of the propellant and inhibit medium-high frequency oscillatory combustion in the engine [5,6]. However, the ignition temperature of aluminum is relatively high and its oxide has an obstructing effect on the combustion reaction, which leads to low combustion efficiency and is prone to problems such as delayed ignition and incomplete combustion [7–9]. During the combustion process of aluminum-containing composite solid propellant, due to the difficulty of aluminum to reach full combustion, two-phase flow loss occurs when it flows out of the nozzle, resulting in engine-specific impulse efficiency reduction and slag deposition [10,11]. Therefore, the combustion efficiency of aluminum has a significant impact on the specific impulse and working safety of the engine. Adding low phase transition temperature metal to aluminum to make aluminum-based alloy fuel lowers the ignition temperature of the aluminum powder; thus, deepening the degree of

reaction of aluminum powder is an important technical way to improve the combustion efficiency [12,13].

In recent years, researchers world-wide have carried out a lot of studies around aluminum-based alloy fuels such as Al–Li [14–16], Al–B [17,18], Al–Mg [19,20], Al–Si [21,22], Al–Fe [23,24], Al–Ni [25–27]. These studies demonstrated the potential for the development and application of aluminum-based alloy fuels as combustible agents, with certain advantages in ignition and combustion over pure aluminum powder. Yasmine Aly et al. [28] prepared three binary aluminum-based alloy fuels, Al–Fe, Al–Ni, and Al–Zn, by mechanical ball milling; the results of thermal analysis and heated wire ignition experiments showed that Zn and Ni oxidized selectively at low temperatures before Al, and the ignition temperatures of the three alloys were lower than that of pure aluminum powder. Later Yasmine Aly et al. [20,29] prepared Al–Mg alloys by a mechanical method and studied their oxidation, ignition, and combustion characteristics; the results showed that the mechanical alloy Al–Mg undergoes the oxidation of Mg followed by the oxidation of Al during the thermal decomposition process and that the ignition temperature of Al–Mg alloys is much lower than that of Al. Cai Shuizhou et al. [30,31] prepared Al–Mg–Zr, Al–Mg–Ce, and Al–W alloy fuels with different mass fractions by gas atomization and other methods, investigated their thermo-reactive properties, and showed that the aluminum-based alloys possessed excellent thermo-oxidative activity and oxidative completeness after the addition of Mg, Zr, Ce, and W metals to Al. While most studies focus on oxidation and combustion characteristics of aluminum-based alloy fuel itself, there are few studies on the application of aluminum-based alloy fuel in solid propellant, and a lack of systematic studies comparing the combustion behavior of aluminum-based alloy fuel and aluminum powder in solid propellant.

Mg has a higher reactivity compared to Al, with an ignition temperature of approximately 615 °C [32]. As shown in Table 1 [33], Mg has a lower melting point and boiling point than Al, indicating better ignition characteristics. Zn has the advantages of low melting point, low boiling point, high density, ease in melting and volatilization when heated, and the ability to increase the density of alloy fuel. The combustion calorific value of Si is higher than Al; adding Si to the Al–Mg system is expected to influence the ignition capacity and heat output of the fuel. Therefore, three aluminum-based alloy fuels, Al–Mg, Al–Zn, and Al–Si–Mg, were selected in this study for comparative experiments with pure aluminum powder. Considering the lower calorific value of Mg and Zn compared to Al, their content in the alloy should not be too high, not exceeding 10%. In order to investigate the combustion characteristics of aluminum-based alloy fuels and their positive role in solid propellants, the micro-morphology, phase composition, reaction weight gain, activation energy, ignition, and combustion properties of the fuels were characterized and analyzed. Then, combined with the high solid content of the HTPB propellant formula, the influence of aluminum-based alloy fuels on the comprehensive properties of the propellant was observed, and the alloy fuels with excellent performance were selected for engine test experiments to explore the influence of alloy fuels on the specific impulse and residue rate of solid propellant.

Table 1. Physical properties and combustion heat of materials.

Element	Density/ ($g \cdot cm^{-3}$)	Melting Point/°C	Boiling Point/°C	Combustion Heat/ ($kJ \cdot kg^{-1}$)
Al	2.70	660	2447	31,058
Mg	1.74	650	1090	25,000
Zn	7.14	420	907	5323
Si	2.33	1410	2355	35,214

2. Materials and Methods

2.1. Materials and Instruments

Aluminum-base alloy fuels, average particle size 30 μm, were purchased from Tangshan Weihao Magnesium Powder Co., Ltd. (Tangshan, China). Aluminum powder FLQT1, average particle size 29 μm, was purchased from Angang Industrial Fine Aluminum Powder Co., Ltd. (Anshan, China). Hydroxy-terminated polybutadiene (HTPB), Type III, was purchased from Zibo Qilong Chemical Co., Ltd. (Zibo, China). Ammonium perchlorate (AP), Class B, Type III, was purchased from Xiangfan Dongfang Yuxing High Ammonium Salt Co., Ltd. (Xiangfan, China).

The following instruments and equipment were used: BT-9300H Laser Particle Size Distributor (BETTER, Dandong, China); Plasma 2000 ICP-OES Inductively Coupled Plasma Atomic Emission Spectrometer (ICP) (NCS, Beijing, China; S-4800 Scanning Electron Microscope (SEM) (Hitachi, Tokyo, Japan); D8 Advance X-ray Diffractometer (XRD) (BRUKER, Billerica, Germany); STA 449 F3 Jupiter Synchronized Thermal Analyzer (TG-DSC) (NETZSCH, Selb, Germany); TRHW-7000C Microcomputer Automatic Calorimeter (Henan Hebi Tianrun Instrument Co., Hebi, China); FASTCAM SA5 High Speed Camera (Photron, Tokyo, Japan); SC-300 Infrared Imager (FLIR Systems, Wilsonville, OR, USA); WL-1 Drop Hammer Impact Sensiometer, WM-1 Friction Sensiometer, HT-201B Static Spark Sensiometer (Xian, China); FCY-1A Bursting Point Tester (Hebi Xintai high-tech instrument manufacturing Co., Ltd., Hebi, China); INSTRON5985 Electronic Universal Material Tester (INSTRON, Norwood, MA, USA); MCR Rotational Rheometer (Anton Paar, Graz, Austria); CAMSIZER X2 Multi-functional Particle Size and Morphology Analyzer, (Microtrac Retsch, Dusseldorf, Germany).

2.2. Sample Preparation

Aluminum-based alloy fuels were prepared by the atomization method; the production process is shown in Figure 1. Aluminum ingots and other metal ingots were used as raw materials, and the melting furnace was used to melt the metal. After the raw materials were fully mixed according to a certain ratio, they were transported to the atomization nozzle through the guide tube, atomized into micron-sized fine alloy melt drops, and solidified into micro-nanometer powders in an inert atmosphere. Finally, the alloy powders were screened for appropriate particle sizes through a vibrating sieve machine, tested for the physicochemical properties, and vacuum-packed.

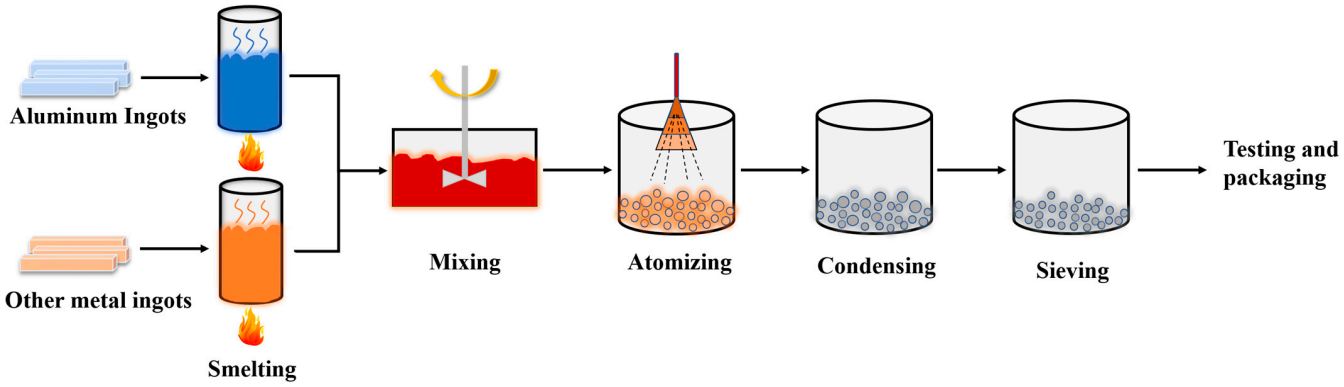


Figure 1. Flow chart of the process of preparing aluminum-based alloy fuel by atomization method.

In order to compare the effects of aluminum-based alloy fuels on propellant performance, propellants with 82% solid content were prepared using the same masses of aluminum-based alloy and aluminum powder, as a combustible agent. This was mixed in a 1 L mixer and cured at 70 °C for 3 days to obtain propellants. The propellants prepared from Al–Mg, Al–Zn, Al–Si–Mg, and Al were numbered as 1#, 2#, 3#, and 4#, respectively. In order to study the effect of aluminum-based alloy fuel on the propellant specific impulse efficiency, the combustible agent content was increased from 17% to 21%; the preferred

Al–Zn alloys, Al–Si–Mg alloys, and reference aluminum powders were used to prepare 88% solid content propellants numbered as 5#, 6#, and 7#, respectively. The propellant formulations are shown in Figure 2.

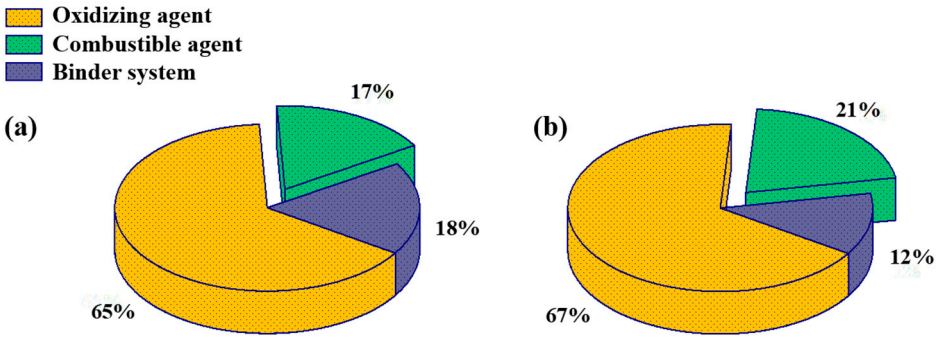


Figure 2. Propellant formulations: (**a**) 82% solid content; (**b**) 88% solid content.

2.3. Experimental Method

A laser particle size distribution instrument and inductively coupled plasma atomic emission spectrometer were used to obtain the particle size and component content of the four fuels, for the calculation of the purity of the samples. Scanning electron microscope and X-ray diffractometer were used to analyze the samples' morphology and composition to determine the alloy phases.

To compare the weight gain rate and activation energy of the samples, they were tested for slow thermal decomposition using a synchronized thermal analyzer, with a temperature increase rate of 10 °C/min, 20 °C/min, and 30 °C/min, a test temperature range of 20–1300 °C, and an inlet rate of 20 mL/min for oxygen and 80 mL/min for nitrogen.

In order to test the ignition ability of fuels, a multi-window combustion test device was used to carry out the ignition experiment, as shown in Figure 3. In a multi-window closed burner, the sample was attached to a nickel-chromium alloy electric ignition wire, and the ignition combustion process was observed through the window with the infrared imager and high-speed camera. Since the powder does not easily adhere to the wire, in order to fix the sample, the ignition wire was made into a spiral shape. The powder sample was first soaked into a paste with ethyl acetate solvent, put into the spiral ignition wire, dried, and then ignited. The combustion heat of fuels was measured by a microcomputer automatic calorimeter under a 3 MPa oxygen environment.

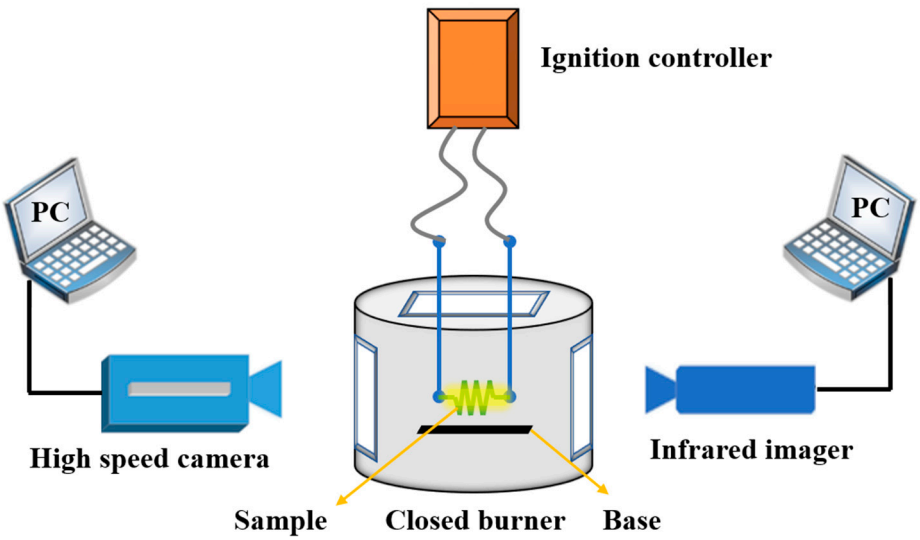


Figure 3. Schematic diagram of multi-window ignition test device.

Various experiments on propellants were conducted according to the Chinese National Experimental Standard [34]. The impact sensitivity was tested according to the impact sensitivity explosion probability method. The drop weight was 2 kg, the fall height was 250 mm, the temperature was 20 °C, and the dosage was 50 mg. The friction sensitivity was tested according to the friction sensitivity explosion probability method. The pressure was 2.45 MPa, the swing angle was 66°, the temperature was 20 °C, and the dosage was 20 mg. The propellant burst point was tested according to the 5-second demurrage method. Electrostatic sensitivity was measured according to thecomposite solid propellant and other explosive electrostatic spark sensitivity test methods. The charge amount was 30~35 mg, the temperature was 20 °C, and the ambient relative humidity was 50%~60%, and the results were expressed as 50% ignition energy (E_{50}). The propellant density was determined according to the density determination method of composite solid propellant, lining, and insulation materials. Using the heat of detonation and heat of combustion constant temperature method, the propellant heat of detonation was measured. Using the burning rate underwater acoustic emission method, the burning rate and pressure index of burning rate were obtained. Using the maximum tensile method, the maximum tensile strength, maximum elongation, and elongation at break were measured. The viscosity of the propellant was tested according to the rotation method. The diameter of the rotating plate was 25 mm, the gap of the plate was 2 mm, and the shear force was set at 60 Pa.

By comparing the effects on propellant mechanical and safety properties, process suitability, and combustion performance, after replacing the ordinary aluminum powder with aluminum-based alloy fuel, the preferred aluminum-based alloy provided the basis for the research of the high solid content high-performance HTPB propellant. The static ground ignition test system of a small solid rocket engine was used to carry out the engine ignition test. The internal residue of the engine was collected for weight comparison, particle size analysis, and active aluminum analysis, to compare the combustion of the propellant. The particle size was characterized by a multi-functional particle size and morphology analyzer, and the particle size corresponding to a cumulative particle size distribution percentage of 50% (D_{50}) and the particle size distribution curve were determined by dry measurement. The activated aluminum was determined according to the redox method, in which activated aluminum reduces iron sulfate to ferrous sulfate in an acidic medium, and titrated with potassium dichromate standard solution using diphenylamine sulfonic acid as an indicator.

3. Results Analysis

3.1. Morphology and Composition of Aluminum-Base Alloy Fuels

The particle sizes and compositions of the three aluminum-based alloy fuels and the reference aluminum powder are shown in Table 2. From the results, it can be seen that the D50 of the samples is between 26 and 34 μm, which is consistent with the specifications. The purity was calculated from the main component contents of the samples, and the purity of all four samples was greater than 98%, which allowed for performance comparison.

Table 2. Sample size and composition.

Sample	D_{50}/μm	Composition/%				Purity/%
		Al	Mg	Zn	Si	
Al–Mg	33.54	88.64	9.48	0	0.0069	98.12
Al–Zn	27.63	89.15	0	10.74	0.035	99.89
Al–Si–Mg	26.52	92.30	0.5	0	7.1	99.9
Al	28.46	99.45	0	0	0	99.45

The microscopic morphology of the four samples is shown in Figure 4a–d, the samples showed a good spherical structure; spherical fuel in solid propellant was favorable for the fluidity of the slurry, and had better process performance. The presence of a small number of ellipsoidal particles in the samples indicated that the samples were affected by the airflow during the jet-curing process. The XRD of the aluminum-based alloy fuels is

shown in Figure 4e. The alloy phase of Al–Mg alloy was Mg_2Al_3, the alloy phase of Al–Zn alloy was $Al_{0.403}Zn_{0.597}$, and the alloy phase of Al–Si–Mg alloy was Al_9Si. The intensity of the diffraction peaks reflected that Al was the dominant phase and the content of alloy phases was low.

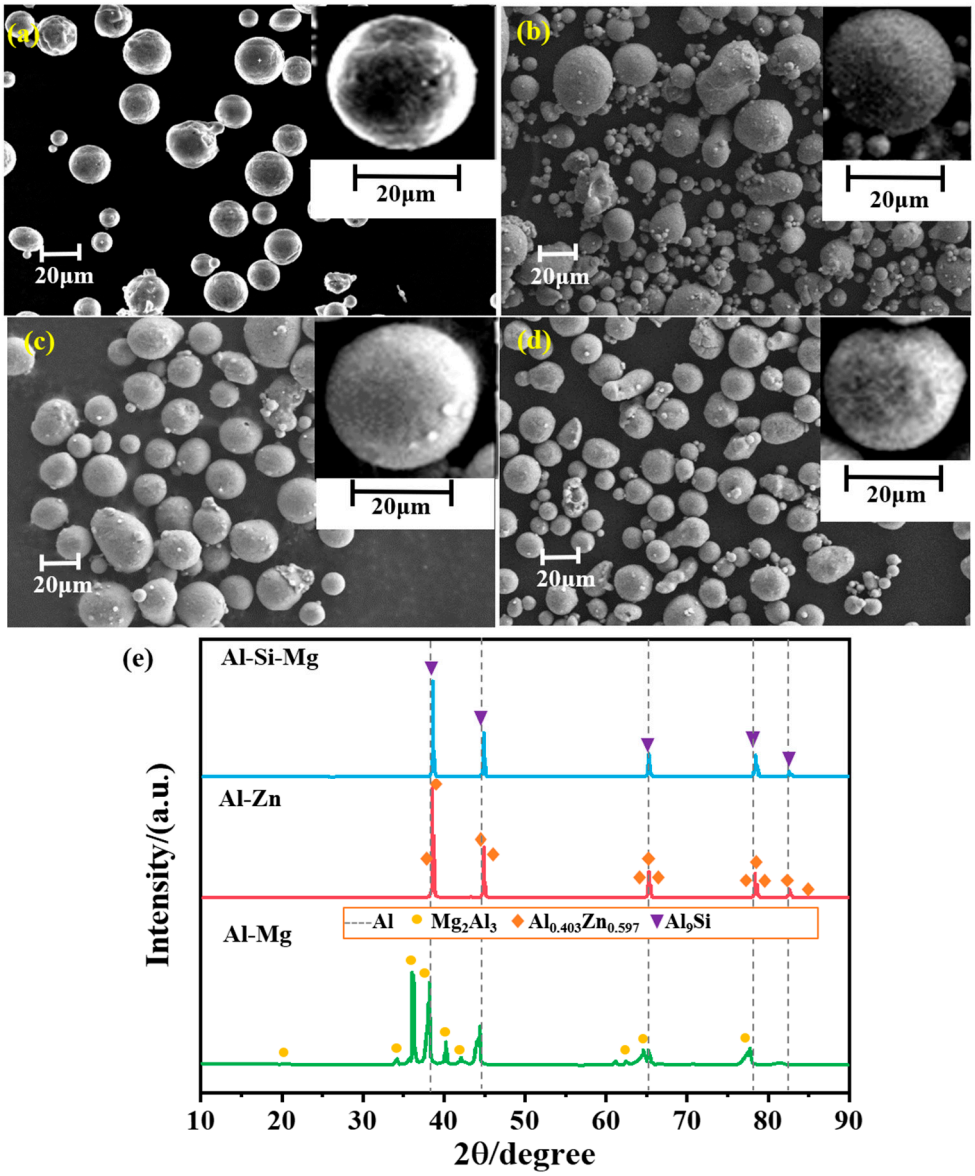


Figure 4. SEM images and XRD patterns of the samples: (**a**) Al–Mg alloy; (**b**) Al–Zn alloy; (**c**) Al–Si–Mg alloy; (**d**) Al powder; (**e**) XRD patterns.

3.2. Thermal Reaction Weight Gain and Activation Energy of Aluminum-Base Alloy Fuels

The result of the thermogravimetric analysis of the four fuels, in Figure 5, shows the weight gain rate of the samples at a temperature increase rate of 10 °C/min. It was found that the weight gain rates of the aluminum-based alloys were significant. The weight gain of the Al–Mg alloys was as high as 84%, which indicated that the addition of the active metal could enhance the oxidation reaction of Al. By differential scanning calorimetry test under air atmosphere, it was found that all four fuels underwent oxidation exothermic reactions at 1000–1200 °C. Al–Mg and Al–Zn alloys were oxidized more deeply because of the high content of the active metal.

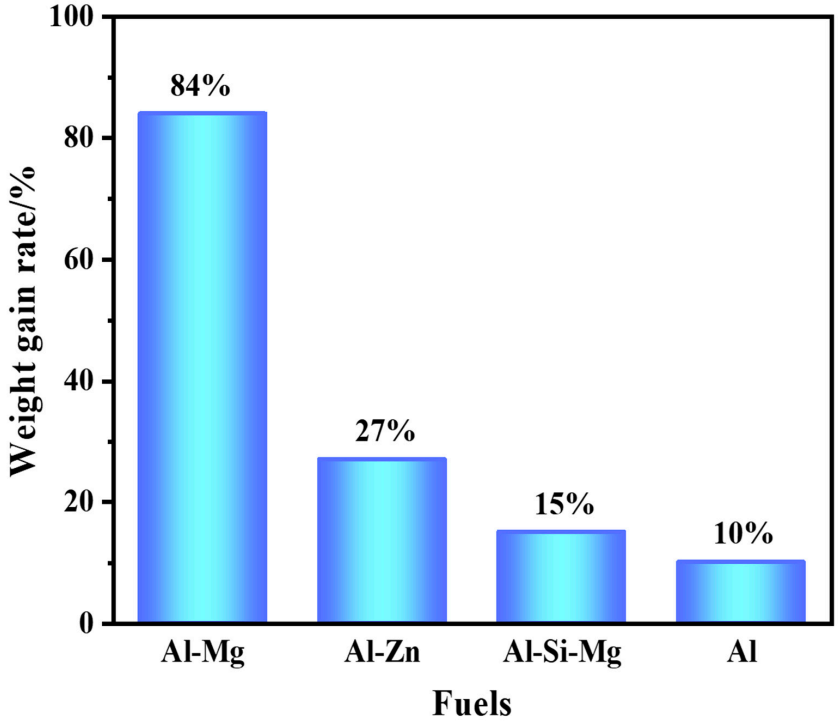


Figure 5. Weight gain rate of fuels.

In order to further investigate the ease with which oxidation reactions occur in fuels, the oxidation kinetic parameters of aluminum-based alloys and aluminum powder were determined comparatively, the activation energy of oxidation was calculated based on Kissinger's method [35] (Equation (1)) and Ozawa's method [36] (Equation (2)) with the following equations:

$$\ln\left(\frac{\beta}{T_p^2}\right) = \ln\left(\frac{AR}{E_k}\right) - \frac{E_k}{RT} \quad (1)$$

and

$$\lg\beta = \lg\left(\frac{AE_o}{RG(\alpha)}\right) - 2.315 - 0.4567\frac{E_o}{RT} \quad (2)$$

where β is the heating rate, °C·min^{-1}; T_p is the peak temperature, °C; A is the finger front factor, s^{-1}; R is the ideal gas constant, 8.314 J·mol^{-1}·K^{-1}; E_k and E_o are the apparent activation energies, kJ·mol^{-1}; T is the temperature, K; $G(\alpha)$ is the integral modeling function; and α is the reaction conversion rate. The calculated results are shown in Table 3. R_k and R_o are the correlation coefficients, the activation energies calculated by Kissinger's and Ozawa's methods were very similar, and, compared to the activation energy of the aluminum powder oxidized in air atmosphere, the activation energies of aluminum-based alloys for oxidation were significantly lower. This indicated that the addition of the active metal lowered the energy threshold required for the oxidation of the aluminum powder, and played a positive role in catalyzing the reaction of aluminum powder.

Table 3. Reaction activation energy of fuels.

Sample	T_p/°C			E_k/(kJ·mol^{-1})	R_k	E_o/(kJ·mol^{-1})	R_o
	β = 10	β = 20	β = 30				
Al–Mg	1175.3	1204.2	1224.1	383.08	0.99	387.56	0.99
Al–Zn	1018.1	1056.7	1080.5	233.95	0.99	243.35	0.99
Al–Si–Mg	1059.5	1083.8	1129.5	208.98	0.95	220.37	0.94
Al	1042.6	1060.9	1068.8	582.17	0.99	574.60	0.99

3.3. Ignition and Combustion Performance of Aluminum-Based Alloy Fuels

Ignition experiments were carried out on four fuels in air, at atmospheric pressure. It was found that only the Al–Mg alloy ignited successfully, emitted a bright flame, and burned stably, while the other three fuels did not ignite. Considering that it might be due to the relatively low oxygen content in the air, in order to further compare the ignition difficulty of the alloy fuels, Al–Zn alloy, Al–Si–Mg alloy, and Al powder were mixed with AP at 1:1, respectively, and then ignition tests were conducted. After mixing AP, the ignition phenomenon occurred in Al–Si–Mg alloy, while Al–Zn alloy and Al powder remained unignited. This was attributed to the fact that Al–Si–Mg alloy contained 0.5% Mg, which improved the ignition responsiveness of the powders. The violent combustion phenomenon of the Al–Si–Mg alloy, in the presence of AP and increased oxygen content, indicated that the ignition responsiveness of the same aluminum-based alloy in the presence of oxygen-containing environments is altered, and the ignition ability is enhanced with the increase of oxygen content.

Examining the ignition experiment of Al–Mg alloy and Al powder in air, the ignition state of fuels was monitored by an infrared imager as shown in Figure 6a. With the increase of heating time, the temperature of the electric heating wire gradually increased and the color became red. The Al–Mg alloy particles rapidly flew away from the ignition wire, and an obvious combustion phenomenon occurred in the air. The time was noted from when the wire temperature reached the background temperature (600 °C). At 4040 ms after, the Al–Mg alloy reached the highest combustion temperature of 1457 °C. In contrast, the Al powder heated for 4120 ms, its temperature was maintained at 944 °C, and the sample combustion phenomenon was not seen, indicating that the addition of Mg can enhance the Al powder combustion.

Through exponential fitting, the ignition temperature change curves of fuels in air are shown in Figure 6b. As can be seen from the figure, only the Al–Mg and Al–Si–Mg + AP fuels have maintained a high heating rate, and the final temperatures reached the ignition zone, successfully realizing the ignition. However, the remaining fuels showed a decreasing trend in the heating rate, absorbing part of the heat when they were heated up, and not reaching the ignition zone. By observing the slopes of the temperature rise curves of four fuels in the middle of the ignition in Figure 6c, it can be seen that the basic law of the temperature rise rate is as follows: Al–Si–Mg = Al–Mg > Al–Zn > Al. Combined with the results of the ignition experiments after the air and the mixed AP, it is concluded that the reliability of fuel ignition under oxygen-poor conditions is in the following order: Al–Mg > Al–Si–Mg > Al–Zn > Al.

According to the combustion heat of metals in Table 1 and the composition content of alloys in Table 2, the theoretical combustion heat values of the fuels were calculated (Equation (3)).

$$Q_T = \sum Q_i \times w_i, \quad i = 1, 2, 3 \tag{3}$$

where Q_T is the theoretical combustion calorific value, kJ·kg^{-1}; Q_i is the theoretical combustion calorific value of each fuel component, kJ·kg^{-1}; and w_i is the percentage of each component of the fuel, %. The actual combustion heat value of fuels was determined, and the combustion efficiency was calculated as:

$$\eta_c = Q_A / Q_T, \tag{4}$$

where η_c is combustion efficiency, % and Q_A is the measured average calorific value, kJ·kg^{-1}. The results are shown in Table 4. The measured average combustion calorific values, ordered from high to low are: Al–Si–Mg > Al–Mg > Al > Al–Zn, the combustion efficiencies, ordered from high to low are: Al–Si–Mg > Al–Mg > Al–Zn = Al, the density calorific values, ordered from high to low are: Al–Si–Mg > Al > Al–Mg > Al–Zn. Based on the above three points, Al–Si–Mg alloy generally shows the characteristics of high calorific value and efficient combustion, and the comprehensive combustion performance is the best.

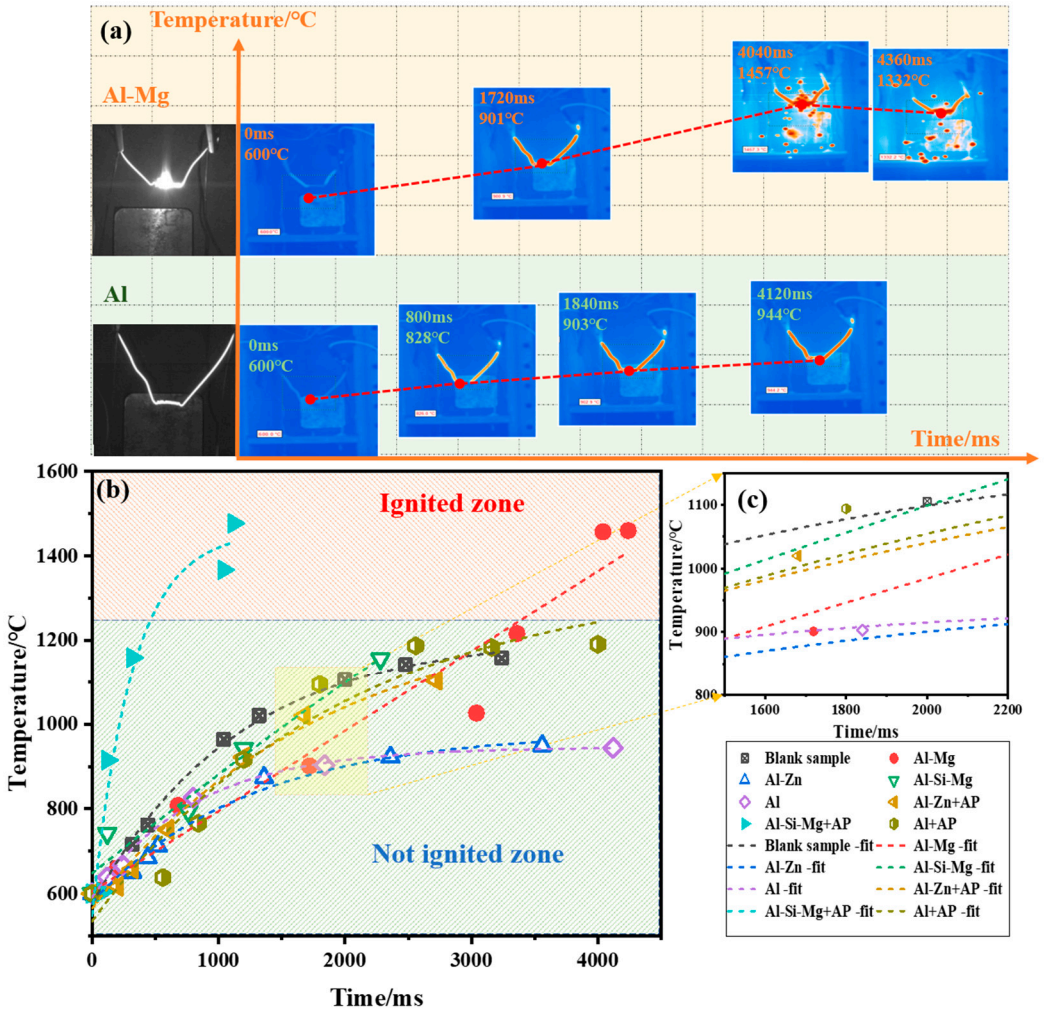


Figure 6. Fuel ignition state and temperature change: (**a**) Ignition state of Al–Mg alloy and Al powder; (**b**) Ignition temperature change curves; (**c**) Enlarged curves.

Table 4. The calorific value of fuels.

Sample	Q_T/(kJ·kg^{-1})	Q_A/(kJ·kg^{-1})	η_c/%	Density/(g·cm^{-3})	Density Calorific Value/(kJ·cm^{-3})
Al–Mg	29,926	29,161	97.4	2.56	74.7
Al–Zn	28,296	25,694	90.8	2.82	72.5
Al–Si–Mg	31,317	30,578	97.6	2.61	79.8
Al	30,914	28,084	90.8	2.68	75.3

3.4. Application of Aluminum-Based Alloy Fuels in Solid Propellant

3.4.1. Mechanics and Safety Performance

When the shell volume and propellant specific impulse of a solid rocket engine are fixed, a larger total impulse is obtained with increased propellant density, as this controls the propellant charge in this situation. Therefore, large propellant density is generally desired, as it is conducive to increasing the total impulse of the engine. In order to investigate the effect of aluminum-based alloys on the mechanical properties of the propellant, the functional components that affect the mechanical properties, such as bonding agents, adhesives, and network modifiers, were not added to the system, so the propellant maximum tensile strength (σ_m), maximum elongation (ε_m), and elongation at break (ε_b) were tested. The sensitivity and bursting point are important parameters that characterize the safety performance of the propellant. To further investigate the effect of aluminum-based

alloys on the safety performance of the propellant, the friction sensitivity, impact sensitivity, electrostatic sensitivity (E_{50}) and burst point temperature (T_F) of propellants were determined. The results of electrostatic sensitivity (E_{50}), burst point temperature (T_F), density (ρ), maximum tensile strength (σ_m), maximum elongation (ε_m), and elongation at break (ε_b) are shown in Figure 7.

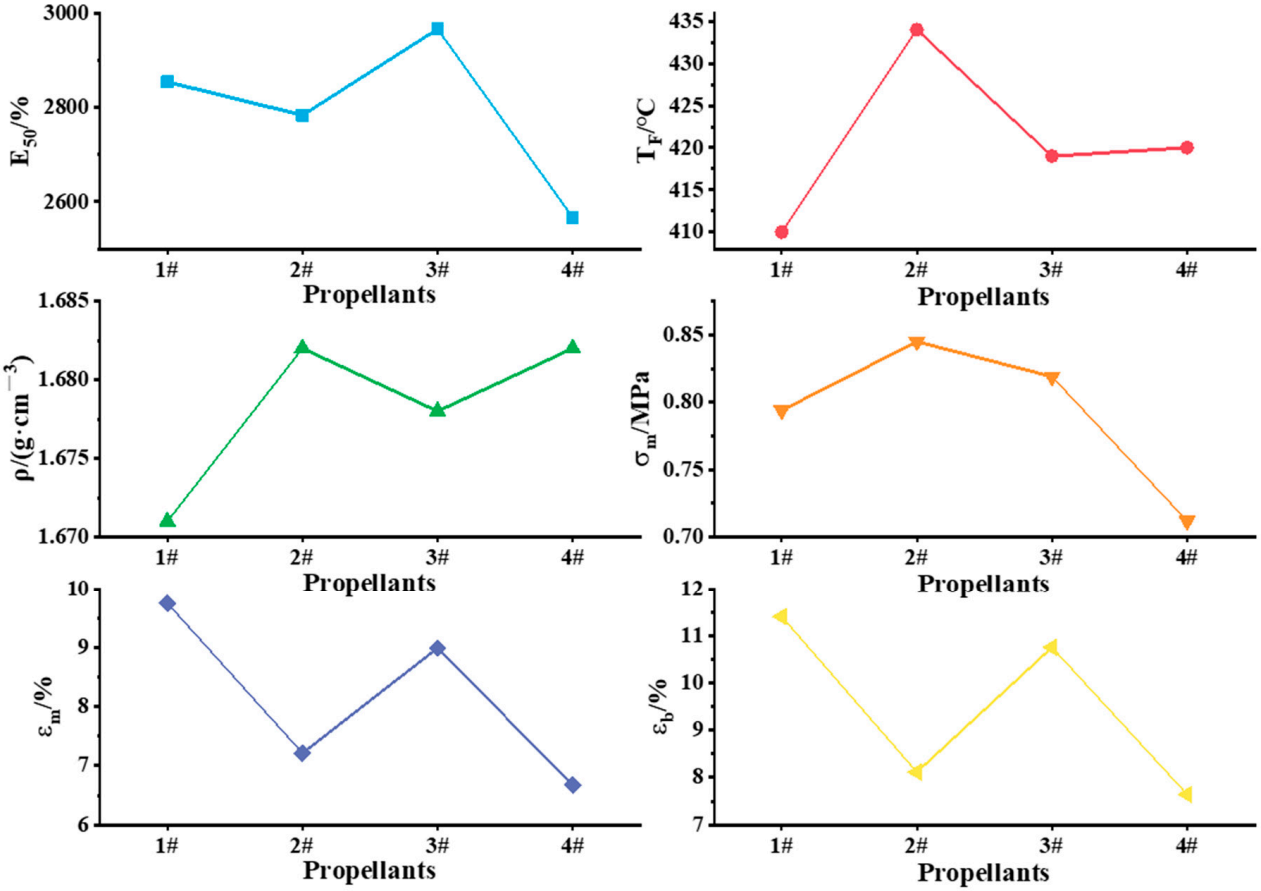


Figure 7. Mechanical and safety properties of propellants.

The friction sensitivity and impact sensitivity of the propellants were tested according to the explosion probability method; for each propellant, friction sensitivity was 1#: 52%, 2#: 84%, 3#: 80%, and 4#: 16%. The impact sensitivities of the four propellants did not differ much, except that the impact sensitivity of propellant 2# was 4%, while the impact sensitivity of the other propellants was 0%. After the addition of active metals, the critical energy of the "hot spot", where an explosive reaction could occur in the propellant, was reduced; therefore, the friction sensitivities of the propellants prepared by aluminum-based alloys were higher (the friction sensitivity of the high burning rate HTPB propellant reached 90%, and still met the safety control measures requirements). When the propellant was subjected to the same external excitation energy, it was easier to form "hot spots", which led to an increase in the friction sensitivity of the propellant.

As can be seen from Figure 7, the E_{50} of propellants 1#~3# is higher than that of 4#, indicating that the electrostatic sensitivity of the solid propellants was reduced by the addition of aluminum-based alloys. The burst point temperatures of the four propellants did not differ much. However, as thermal sensitivity increases with lower burst point temperature, the propellant prepared with the Al–Mg alloy had a higher thermal sensitivity. The densites of propellants 2# and 4# were comparable, and the density of propellant 1# was the lowest. Therefore, considering the performance of the propellant, the content of Mg in the alloy should not be too high. The maximum tensile strength (σ_m), maximum elongation (ε_m), and elongation at break (ε_b) were better for the propellants prepared from

aluminum-based alloys than for those prepared from aluminum powder. These results indicate that the addition of aluminum-based alloys effectively improved the mechanical properties of solid propellants.

3.4.2. Process Adaptability

The process performance of the propellant directly determines the propellant castability, which greatly affects the success of the propellant charge. Therefore, better process performance can meet the use requirements of propellant. Generally, viscosity is used to characterize the process performance of propellant, and the growth index of viscosity over time can represent the growth rate of propellant viscosity, as follows:

$$\eta = at^n, \tag{5}$$

where η is viscosity, Pa·s; a refers to the pre-exponential factor; t is time, h; n is the growth index of viscosity. The value of the pre-exponential factor represents the initial viscosity of slurry at the end of mixing. When its value is too high, this affects the fluidity and the pouring of propellant. If the growth index of viscosity is too large, it means that the viscosity grows fast, the viscosity increases significantly in a short time, and the service life will be shortened, resulting in the inability for the propellant to be poured.

Table 5 shows the viscosity of the four propellants at different times. The viscosities were at the same level, and in general, the solid propellant slurry pre-exponential factor and viscosity growth index were small, and no significant deterioration of process performance was seen. Therefore, the addition of aluminum-based alloys had a small effect on the viscosity of solid propellants and did not affect their performance.

Table 5. The viscosity of propellants at different times.

Number	η/(Pa·s)						a	n
	0.5 h	1 h	1.5 h	2 h	2.5 h	3 h		
1#	296	354	385	409	488	520	273	0.22
2#	260	294	349	384	432	472	234	0.24
3#	203	238	261	284	314	351	188	0.21
4#	295	344	364	392	435	487	274	0.22

3.4.3. Combustion Performance

The heat of combustion can characterize the energy level of propellant prepared from an alloy fuel; thus, the burning rate is an important parameter to characterize the combustion performance of solid propellant, and the burning rate pressure exponent is one of the important indices that characterize the combustion stability of propellant [37]. The combustion performance of the propellant measured by the constant temperature method and underwater acoustic emission method is shown in Figure 8.

Five heat of combustion tests were performed for each propellant and averaged. As shown in Figure 8a, the scatter points are the test values and the bars show the average values. it was found that the heat of combustion of propellants 1#~3# were significantly increased compared with that of propellant 4#, and the highest heat of combustion of propellant 1# was increased by 8.5%, propellant 2# was increased by 7.1%, and propellant 3# was increased by 5.9%. As shown in Figure 8b, the burning rate of propellants 1#~3# increased with increasing pressure, and the pressure exponents of the four propellants were comparable. The results of the heat of combustion and burning rate showed that the combustion performance of the propellant was significantly improved after the introduction of Mg, Zn, and Si into Al. Moreover, although the combustion performance of Si was slightly worse than that of Mg and Zn, the Al–Si–Mg alloy combined the high calorific value of Si and the easy ignition of Mg, and showed a good level of performance in terms of calorific value and burning rate; thus, the Al–Si–Mg alloy had a certain advantage in improving the specific impulse of propellant.

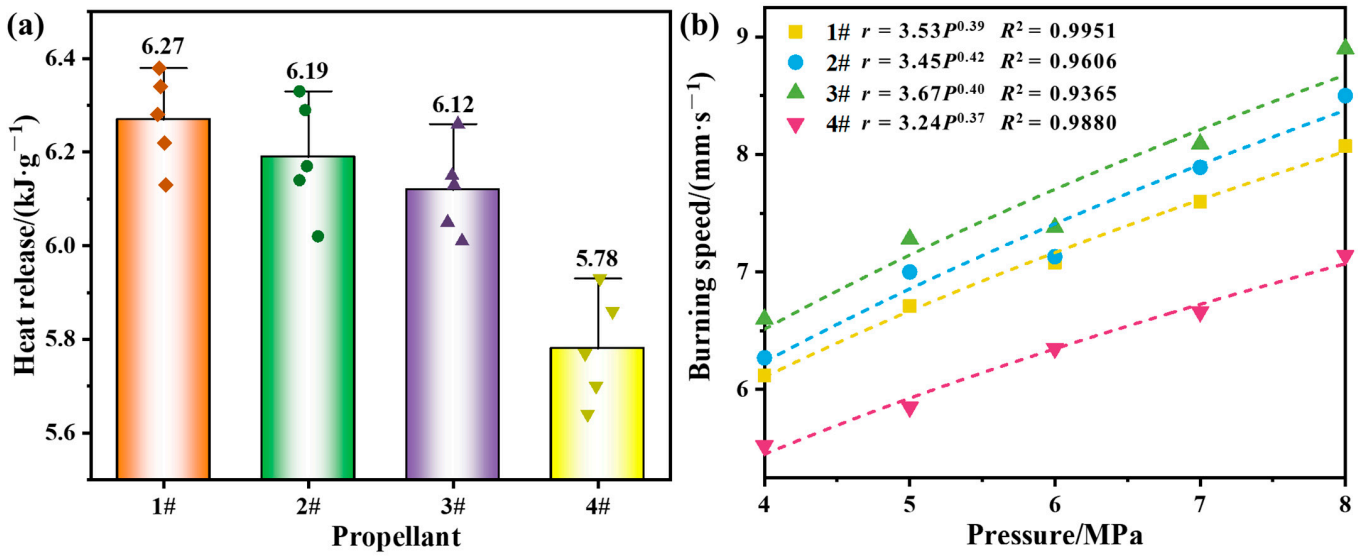


Figure 8. Propellant combustion performance: (**a**) heat of combustion; (**b**) burning rate curves.

3.4.4. Engine Ignition Test

According to the above study, it was found that all the aluminum-based alloy fuels resulted in higher propellant friction sensitivity, calorific value, and burning rate, which are favorable for propellant combustion. However, because Mg has a low density, it is not favorable to increase the total impulse of the propellant. Considering the energy of propellant comprehensively, the content of Mg in alloy should not be too high, so three kinds of fuels, Al–Zn, Al–Si–Mg alloys, and Al powder, were selected for comparative study, and propellants 5#, 6#, and 7# were prepared to verify whether aluminum-based alloy fuels effectively improve the specific impulse efficiency of HTPB propellant.

The high solid propellant slurries prepared from three fuels are shown in Figure 9a; all slurries had bright surfaces and good fluidity. The three cured propellants are shown in Figure 9b; the cut propellant surfaces were all dense and free of defects. The standard engine ground ignition test was performed on the propellants. After the test, the residues on the inner wall of the casing were collected as shown in Figure 9c. The residue on the nozzle convergence section and the top cover is shown in Figure 9d, and the ignition test process is shown in Figure 9e. The ground static ignition test curve of the three engines is shown in Figure 9f, and the result of the particle size analysis of the fine residue is shown in Figure 9g.

The results of the three engines' ground static ignition test are shown in Table 6. The specific impulse efficiency of propellant 5# was slightly higher than that of propellant 7#, but the measured specific impulse of 5# was lower than that of 7# because of the lower calorific value of Zn. The measured specific impulse and the specific impulse efficiency of propellant 6# were slightly higher than that of propellant 7#, mainly because of the high calorific value and rapid combustion of the Al–Si–Mg alloy. The Al–Si–Mg alloy was equivalent to adding approximately 0.5% Mg and 7% Si into Al, and while Si had a higher heat of combustion than Al, Si alone was insufficient to improve the ignition and promote the combustion of Al powder. The Al–Si–Mg alloy made full use of the advantages of a small amount of Mg ignition to make up for the shortcomings of Si, so that it had both good ignition and combustion performance, and therefore, the specific impulse of its charging engine was the highest.

Table 6. Results of engine ignition test.

Number	Fuel	Corrected to 7 MPa Specific Impulse/(N·s·kg^{-1})		Specific Impulse Efficiency/%
		Theoretical Value	Measured Value	
5#	Al–Zn	261.9	235.7	90.00
6#	Al–Si–Mg	265.6	238.0	89.61
7#	Al	265.6	237.5	89.42

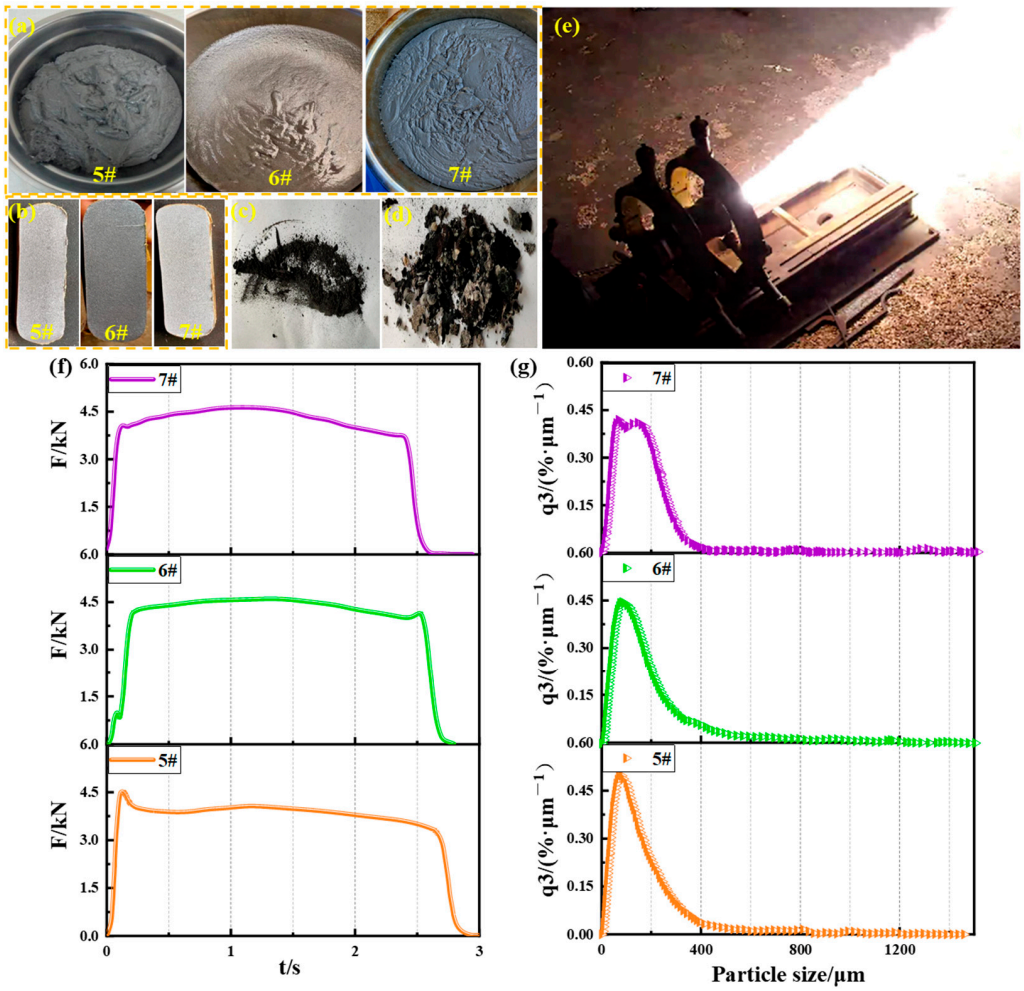


Figure 9. Propellant engine ignition test: (**a**) propellant slurries; (**b**) cured propellants; (**c**) engine casing inner wall residue; (**d**) engine top cover and nozzle convergence section inner wall residue; (**e**) engine test process; (**f**) F-t curves; (**g**) residue particle size distribution curves.

Since most of the fine solid products fly out of the engine with the high-temperature hot gas flow when the solid engine is in operation, only a small amount of residue remains in the solid engine; however, the combustion efficiency of the propellants can be compared by characterizing the residues in the casing after the test run. The weight of the residue and its active aluminum content indicate the degree of combustion of aluminum powder, and the degree of residue scouring of the nozzle is characterized by the change of the nozzle throat diameter. The statistics of the amount of residue in the inner wall, the amount of residue in the top cover and convergence section, the fine residue particle size (D_{50}), the active aluminum content, and the enlargement of the throat diameter after test scouring of engine test are shown in Table 7.

Table 7. Engine residue analysis and throat diameter change.

Number	Residue on the Inner Wall/g	Residue on the Top Cover and Convergence Section/g	D_{50}/μm	Active Aluminum Content/%	Throat Diameter/mm		
					Pre-Test	Post-Test	Expansion
5#	2.03	6.69	134	3.6	20.90	21.40	0.50
6#	2.31	7.52	147	3.5	20.0	20.58	0.58
7#	3.65	18.25	153	4.1	20.10	20.92	0.82

The residue mass and particle size, active aluminum content, and throat diameter change of propellants 5# and 6# were all smaller than those of propellant 7#, indicating that compared to Al powder, Al–Zn alloy and Al–Si–Mg alloy had favorable characteristics of little scour on the nozzle, low residue, and full combustion during engine ignition test. These results are of great significance for improving specific impulse efficiency and increasing engine reliability.

4. Conclusions

Using aluminum powder, commonly used in solid propellants, as a reference, this study characterized the physical and chemical properties of three aluminum-based alloy fuels and studied their performance rules when applied to solid propellant. The following conclusions were obtained.

(1) In comparing the ignition ability of four spherical fuels with different compositions and similar particle sizes in an air environment as well as mixed with AP, the Al–Mg alloy had better ignition ability. The order of ignition reliability for the four fuels was Al–Mg > Al–Si–Mg > Al–Zn > Al, i.e., the alloys were easier to ignite than aluminum powder.

(2) The effect of aluminum-based alloys on propellant properties was investigated using HTPB propellant formulations. The results showed that, compared to propellants made from Al powders, propellants prepared from Al–Mg, Al–Zn, and Al–Si–Mg alloys were characterized by higher friction sensitivity, larger combustion calorific value, increased burning rate and pressure exponent, improved mechanical properties, and comparable levels of process properties.

(3) The applied research of propellants with high solid content was carried out for Al–Zn and Al–Si–Mg alloys, and Al powder. Through the engine ignition test, it was found that the specific impulse and specific impulse efficiency of the propellant prepared by Al–Si–Mg alloys were improved. In addition, the propellants prepared by Al–Zn and Al–Si–Mg alloys had less residue, less scouring of the nozzle and more full combustion, which is of important application significance for improving the reliability of engine operation and developing a high-performance HTPB propellant formula.

Author Contributions: Conceptualization, H.X., K.W. and H.R.; methodology, K.W.; software, H.X.; validation, H.X., K.W. and H.R.; formal analysis, H.X. and K.W.; investigation, H.X.; resources, H.R.; data curation, H.X. and K.W.; writing—original draft preparation, H.X. and K.W.; writing—review and editing, H.R.; visualization, H.X.; supervision, Q.J.; project administration, H.R.; funding acquisition, H.R. and Q.J. All authors have read and agreed to the published version of the manuscript.

Funding: This research was funded by the National Natural Science Foundation of China (grant number 21975024).

Data Availability Statement: The data presented in this study are presented in the figures and tables in this article.

Conflicts of Interest: The authors declare no conflict of interest.

References

1. Patil, M.S.; Singh, H. Ballistic and mechanical properties of HTPB based composite propellants. *J. Hazard. Mater.* **1988**, *19*, 271–278. [CrossRef]
2. Miller, M.S.; Holmes, H.E. Subatmospheric burning rates and critical diameters for AP/HTPB propellant. *J. Propuls. Power* **1990**, *6*, 671–672. [CrossRef]
3. Yuan, J.; Liu, J.; Zhou, Y.; Zhang, Y.; Cen, K. Thermal decomposition and combustion characteristics of Al/AP/HTPB propellant. *J. Therm. Anal. Calorim.* **2021**, *143*, 3935–3944. [CrossRef]
4. Mahanta, A.K.; Dharmsaktu, I.; Pattnayak, P.K. Rheological Behaviour of HTPB-based Composite Propellant: Effect of Temperature and Pot Life on Casting Rate. *Def. Sci. J.* **2007**, *57*, 581–588. [CrossRef]
5. Shi-xi, W.U.; Tian-fu, Z.; Chong-yang, Z.; Xiao-ping, L.I.; Qi-wei, H.U. Recent Advances on Applications of New Energetic Ingredients in HTPB Composite Solid Propellants. *Chin. J. Energetic Mater.* **2019**, *27*, 348–355.
6. Liu, M.; Yu, W.; Li, S. Effect of aluminum-based additives on the ignition performance of ammonium perchlorate-based composite solid propellants. *Acta Astronaut.* **2023**, *204*, 321–330. [CrossRef]
7. Toros, S.; Ozturk, F.; Kacar, I. Review of warm forming of aluminum–magnesium alloys. *J. Mater. Process. Technol.* **2008**, *207*, 1–12. [CrossRef]
8. Lloyd, D.J. The deformation of commercial aluminum-magnesium alloys. *Metall. Trans. A* **1980**, *11*, 1287–1294. [CrossRef]
9. Makino, A.; Law, C.K. SHS Combustion Characteristics of Several Ceramics and Intermetallic Compounds. *J. Am. Ceram. Soc.* **1994**, *77*, 778–786. [CrossRef]
10. Tang, Q.; Pang, A.M.; Wang, Y. Research progress analysis of aluminum combustion property and mechanism of solid propellant. *Guti Huojian Jishu/J. Solid Rocket. Technol.* **2015**, *38*, 232–238.
11. Xiao, L.Q.; Fan, X.Z.; Wang, H.; Li, J.Z.; Tang, Q.F. Research Progress on the Agglomeration Phenomenon of Aluminum Powder in the Combustion of Aluminized Solid Propellants. *Huozhayao Xuebao/Chin. J. Explos. Propellants* **2018**, *41*, 7–15, 25.
12. DeLuca, L.; Maggi, F.; Dossi, S.; Weiser, V.; Franzin, A.; Gettwert, V. High-energy Metal Fuels for Rocket Propulsion:Characterization and Performance. *Huozhayao Xuebao/Chin. J. Explos. Propellants* **2013**, *2013*, 14.
13. Deluca, L.T.; Shimada, T.; Sinditskii, V.P.; Calabro, M. *Chemical Rocket Propulsion—A Comprehensive Survey of Energetic Materials*; Springer International Publishing: Berlin/Heidelberg, Germany, 2016.
14. Zhu, P.; Li, J.C.M.; Liu, C.T. Reaction mechanism of combustion synthesis of NiAl. *Mater. Sci. Eng. A* **2002**, *329–331*, 57–68. [CrossRef]
15. Biswas, A.; Roy, S.K.; Gurumurthy, K.R.; Prabhu, N.; Banerjee, S. A study of self-propagating high-temperature synthesis of NiAl in thermal explosion mode. *Acta Mater.* **2002**, *50*, 757–773. [CrossRef]
16. Dyer, T.S.; Munir, Z.A.; Ruth, V. The combustion synthesis of multilayer NiAl systems. *Scr. Metall. Mater.* **1994**, *30*, 1281–1286. [CrossRef]
17. Birol, Y. Aluminothermic reduction of boron oxide for the manufacture of Al–B alloys. *Mater. Chem. Phys.* **2012**, *136*, 963–966. [CrossRef]
18. Liang, D.; Xiao, R.; Liu, J.; Wang, Y. Ignition and heterogeneous combustion of aluminum boride and boron–aluminum blend. *Aerosp. Sci. Technol.* **2019**, *84*, 1081–1091. [CrossRef]
19. Corcoran, A.L.; Wang, S.; Aly, Y.; Dreizin, E.L. Combustion of Mechanically Alloyed AlMg Powders in Products of a Hydrocarbon Flame. *Combust. Sci. Technol.* **2015**, *187*, 807–825. [CrossRef]
20. Aly, Y.; Dreizin, E.L. Ignition and combustion of Al·Mg alloy powders prepared by different techniques. *Combust. Flame* **2015**, *162*, 1440–1447. [CrossRef]
21. Parimi, V.S.; Huang, S.; Zheng, X. Enhancing ignition and combustion of micron-sized aluminum by adding porous silicon. *Proc. Combust. Inst.* **2017**, *37*, 2317–2324. [CrossRef]
22. Shi, Y.A.N.; Bing, P.A.N.; Qing-qing, Y.; Jia-peng, W.; Qing-jie, J.; Feng-zhen, D.U. Preparation and Reaction Characteristics of Spherical Al-Si Alloy Fuel. *Chin. J. Energetic Mater.* **2020**, *28*, 766–772.
23. Kou, Y.; Wang, Y.; Zhang, J.; Guo, K.-G.; Song, X.-L. Iron/aluminum nanocomposites prepared by one-step reduction method and their effects on thermal decomposition of AP and AN. *Def. Technol.* **2023**, *22*, 74–87. [CrossRef]
24. Sui, H.; Atashin, S.; Wen, J.Z. Thermo-chemical and Energetic Properties of Layered Nano-thermite Composites. *Thermochim. Acta* **2016**, *642*, 17–24. [CrossRef]
25. Vummidi, S.L.; Aly, Y.; Schoenitz, M.; Dreizin, E.L. Characterization of Fine Nickel-Coated Aluminum Powder as Potential Fuel Additive. *J. Propuls. Power* **2010**, *26*, 454–460. [CrossRef]
26. Seropyan, S.; Saikov, I.; Andreev, D.; Saikova, G.; Alymov, M. Reactive Ni–Al-Based Materials: Strength and Combustion Behavior. *Met.-Open Access Metall. J.* **2021**, *11*, 949. [CrossRef]
27. Mason, B.A.; Groven, L.J.; Son, S.F. The role of microstructure refinement on the impact ignition and combustion behavior of mechanically activated Ni/Al reactive composites. *J. Appl. Phys.* **2013**, *114*, 181. [CrossRef]
28. Aly, Y.; Schoenitz, M.; Dreizin, E.L. Aluminum-Metal Reactive Composites. *Combust. Sci. Technol.* **2011**, *183*, 1107–1132. [CrossRef]
29. Aly, Y.; Schoenitz, M.; Dreizin, E.L. Ignition and combustion of mechanically alloyed Al–Mg powders with customized particle sizes. *Combust. Flame* **2013**, *160*, 835–842. [CrossRef]
30. Li, L.F.; Cai, S.Z.; Xu, C.J.; Fu, H.; Zou, H. Preparation and Performance of High Reactive Al-Mg-Zr Alloy Fuels with Intensive Heat Release. *Chin. J. Energetic Mater.* **2016**, *24*, 137–143.

31. Yi, H.; Cai, S.; Hui, Z. Effect of Rare Earth Ce on Thermal Performance of Al-Mg-Ce Alloy Fuels. *Rare Met. Mater. Eng.* **2018**, *47*, 1185–1191.
32. Murray, J.L.; McAlister, A.J. The Al-Si (Aluminum-Silicon) system. *Bull. Alloy Phase Diagr.* **1984**, *5*, 74–84. [CrossRef]
33. Zhang, J.K.; Zhao, F.Q.; Qin, Z.; Li, H. Research Progress of Al-based Alloy Fuels and Perspectives for Applications in Solid Propellants. *Chin. J. Explos. Propellants* **2023**, *46*, 101–116.
34. *GJB 772A-92*; Explosive Test Method. COSTIND: Beijing, China, 1997.
35. Kissinger, H.E. Reaction Kinetics in Differential Thermal Analysis. *Anal. Chem.* **1957**, *29*, 1702–1706. [CrossRef]
36. Ozawa, T. A New Method of Analyzing Thermogravimetric Data. *Bull. Chem. Soc. Jpn.* **1965**, *38*, 1881–1886. [CrossRef]
37. Wang, J.; Yang, H.; Cheng, L.; Gao, P.; Li, Y.; Song, D. Ignition and Combustion Characteristics of B/NC/CuO Thermite Microparticles. *Metals* **2022**, *12*, 1419. [CrossRef]

Disclaimer/Publisher's Note: The statements, opinions and data contained in all publications are solely those of the individual author(s) and contributor(s) and not of MDPI and/or the editor(s). MDPI and/or the editor(s) disclaim responsibility for any injury to people or property resulting from any ideas, methods, instructions or products referred to in the content.